Formation and Evolution of Galaxy Outskirts
Proceedings IAU Symposium No. 321, 2016
A. Gil de Paz, J.H. Knapen & J.C. Lee, eds.
© International Astronomical Union 2017
doi:10.1017/S1743921316009194

Ultra-deep imaging of nearby galaxy outskirts from the ground

Ignacio Trujillo[1,2]

[1]Instituto de Astrofísica de Canarias, c/ Vía Láctea s/n, E-38205, La Laguna, Tenerife, Spain
[2]Departamento de Astrofísica, Universidad de La Laguna, E-38206, La Laguna, Tenerife, Spain
email: trujillo@iac.es

Abstract. We show how present-day 10 meter class telescopes can provide broadband imaging 1.5-2 mag deeper than most previous results within a reasonable amount of time (∼8h on source integration). We illustrate the ability of the 10.4 m Gran Telescopio de Canarias (GTC) telescope to produce imaging with a limiting surface brightness of 31.5 mag/arcsec^2 (3σ in 10×10 arcsec boxes). We explore the stellar halos of nearby galaxies obtaining surface brightness radial profiles down to $\mu_r \sim$33 mag/arcsec^2. This depth is similar to that obtained using star counts techniques of Local Group galaxies, but is achieved at a distance where this technique is unfeasible.

Keywords. galaxies: evolution – galaxies: formation – galaxies: halos – galaxies: photometry – galaxies: spiral

1. Introduction

Using the star counts technique, the exploration of nearby galaxies has revealed features with equivalent surface brightness of ∼31-32 mag/arcsec^2 (e.g. McConnachie *et al.* 2009, Ibata *et al.* 2009). This impressive surface brightness is ∼2 magnitudes deeper than current very deep imaging using broadband filters (e.g. Mihos *et al.* 2005, Jablonka *et al.* 2010, Martínez-Delgado *et al.* 2010, Ferrarese *et al.* 2012, Duc *et al.* 2015, Fliri & Trujillo 2016). However, the technique of resolved star counts is not free of important problems: a) it can not be applied very far away (typically up to 16 Mpc using HST; Zackrisson *et al.* 2012), b) the population of stars that this technique traces depends on the distance and c) background (distant galaxies) and foreground (stars of our own Galaxy) contaminants are not straightforward to remove. With the star counting technique, the volume that can be explored is quite limited, and consequently also the number and the type of galaxies that can be studied.

Exploring very low surface brightness structures around galaxies is key for testing the ΛCDM galaxy formation scenario. According to this model all present-day galaxies will show several streams and a prominent extended stellar halo if they are observed down to $\mu_V >$31 mag/arcsec^2 (e.g. Cooper *et al.* 2010). Present-day limiting surface brightness using broadband imaging (∼30 mag/arcsec^2) is at the verge for testing this prediction. Considering the intrinsic stochasticity of the stellar halo formation process, the need of a large sample of galaxies is clear if we want to probe the ΛCDM galaxy formation model in depth. The limited number of objects that can be studied by the star count technique forces us to explore whether we can go deeper with integrated photometry, in terms of surface brightness, than previous works.

1.1. *Crossing the 30 mag/arcsec^2 frontier: the challenges*

There are many technical challenges that need to be addressed to obtain broadband imaging showing features fainter than 30 mag/arcsec^2:

https://doi.org/10.1017/S1743921316009194 Published online by Cambridge University Press

• The sky brightness. Even at the darkest spots on earth, where the observatories are located, the night sky brights quite substantially: $\mu_V \sim 22$ mag/arcsec^2. Long time integrations are able to reduce the noise associated to this brightness.

• Internal reflections due to the structure of the telescope and the dome. At $\mu_V \gtrsim 26$ mag/arcsec^2, light reflections on the telescope and dome structure can left their imprints on the image. A way to reduce this problem is the use of telescopes with simple optics (i.e. like Dragonfly; Abraham & van Dokkum 2014) or with a clever observing strategy that prevents the repetitions of similar orientation of the camera on the sky (Trujillo & Fliri 2016).

• Scattered light from nearby sources. Slater *et al.* (2009) have shown that at $\mu_V \sim 29.5$ mag/arcsec^2, an image taken from the ground should have all the pixels of the image affected by the scattered light from nearby bright sources. The way to handle this problem is to have an extremely accurate characterization of the Point Spread Function (PSF) of the camera to correct this effect.

In addition to all the technical challenges described above, an important limitation to the depth of the structures that can be explored is connected to the presence of Galactic cirrus. These cirrus appear everywhere on the sky and, for this reason, a careful selection of sky locations with minimum contamination should be taken.

2. A pilot program with the 10.4m Gran Telescopio de Canarias

2.1. *Data*

Ultra deep observations of the galaxy UGC 00180 and its surrounded region were carried out with GTC using the OSIRIS camera. The images were obtained using the Sloan r' filter during 6 (non-consecutive) nights. Images were taken under good seeing conditions $\sim$0.9 arcsec. We designed an observational strategy that aims to obtain a background as flat as possible around our galaxy target. In addition to conduct the usual dithering scheme, we have carried on a rotation pattern to remove as much as possible effects due to scattered (residual) light contamination. With the rotation pattern, we avoid that a potential reflected residual light (from the telescope dome, telescope structure, etc) affects the camera along the same position angle (P.A.) during the full set of pointings. Moreover, the large number (243) of images we get in the end allow us to build a very flat sky to reach our purpose. The observational strategy is illustrated in Fig. 1. Each pointing of the sequence has an exposure time of 120s. That corresponds to a total amount of time on source of 8.1 hours. A detailed description of the observing strategy can be found in Trujillo & Fliri (2016).

The selection of the target, UGC 00180, was done to assure that the OSIRIS FOV was able to cover a significant region of sky around the galaxy. UGC 00180 redshift is 0.0369. This locates the object at a distance of 151.3 Mpc. A single shot of the OSIRIS camera covers 343×343 kpc at the galaxy distance. UGC 00180 is a Sab massive galaxy (M_B=-21.76, $V_{\rm rot}$=267.6±18.4 km/s). In this sense, this galaxy is comparable with M31. UGC 00180 has R_{25}(B-band)=32±3 arcsec (i.e. 23.5±2.2 kpc). The stellar mass of UGC 00180 is $M_\star \sim 1.3\times10^{11} M_\odot$.

An accurate estimation of the flat field correction is key for the purpose of this work. Masterflats were created for each observing night using a median of the normalized science images of that night. The amount of data is such that there are at least 15 science images every night to combine and create the masterflat of that night. The masterflats have a typical rms of 0.055%. The photometric calibration of our science images is based on the photometry of SDSS DR7. We matched the SDSS DR7 photometric catalogue to

https://doi.org/10.1017/S1743921316009194 Published online by Cambridge University Press

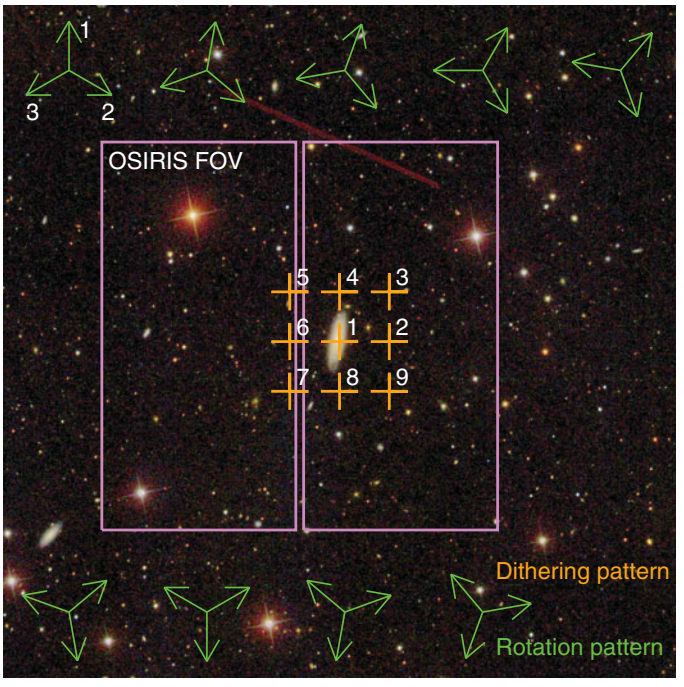

Figure 1. Dithering and rotation sequence followed to get the final image. The background image is a color composite of the UGC 00180 region obtained from SDSS. The field of view of each pointing by the OSIRIS camera (7.8 arcmin×7.8 arcmin) is overplotted with a violet contour. The position of the orange crosses indicate the dithering pattern followed in each block of observations, whereas the green arrow indicates the position angle of the camera in each set of observations. In total, the final image is composed by 3×9×9 pointings. Figure taken from Trujillo & Fliri (2016), reproduced by permission of the AAS.

ours. The typical number of stars that are within each our individual science images to conduct this calibration is ∼30.

The final coadded image (see Fig. 2) is significantly deeper than the individual exposures and low surface brightness features, hidden in the individual exposures, emerge in the final stacking. These low surface brightness features (extended dust emission, halos of bright stars, etc) affect the sky determination of our individual science images. For this reason, it is necessary to mask these regions and repeat the process of the sky determination in the individual exposures. The result of this repetition is our final image.

In our final image, the most conspicuous feature is the extended and filamentary emission observed in the bottom part of the image that we have tentatively tagged as Galactic Cirrus. We have used the Planck satellite to see whether it is possible to see this feature at the 857 GHz (350 μm) channel (Planck Collaboration *et al.* 2014). At this wavelength, the dust of our own Galaxy is particularly visible. Our analysis shows that the position of the maximum emission of the dust at the 857 GHz channel coincides with the spatial location of the extended emission in the optical, suggesting a dust origin for this feature.

2.2. *Surface brightness limit and scattered light*

We have decided to obtain the limiting surface brightness of the image as the equivalent to a 3σ fluctuation (compared to the sky noise) in square boxes of 10 arcsec×10 arcsec. The reason behind using boxes of this size is given by the typical size of the components we are interested to explore in the stellar halo of UGC 00180 (see Fig. 4). At the redshift

https://doi.org/10.1017/S1743921316009194 Published online by Cambridge University Press

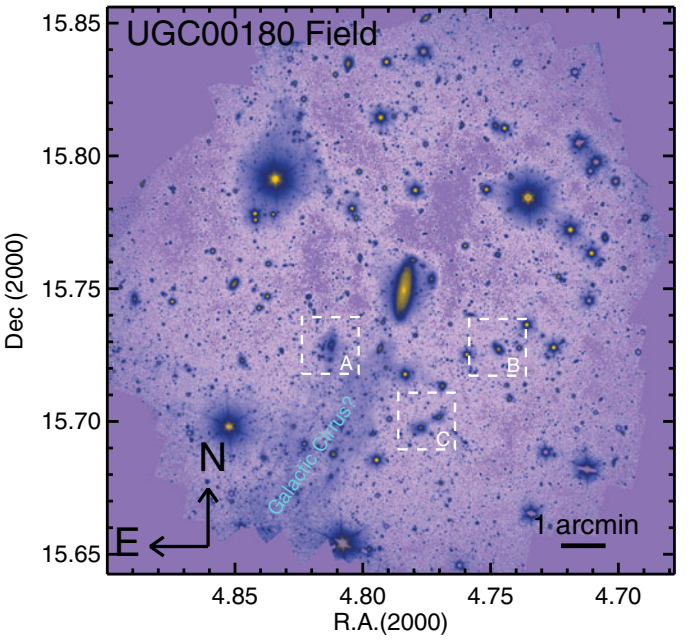

Figure 2. Field of view of 12.7 arcmin×12.7 arcmin around UGC 00180. In addition to our main target, there are a number of interesting astronomical objects that are highlighted. A zoom-in to objects tagged as a), b) and c) is shown in Fig. 3. The presence of an extended and filamentary emission in the bottom part of the image is also tentatively identified as a Galactic Cirrus of our own Galaxy. Figure taken from Trujillo & Fliri (2016), reproduced by permission of the AAS.

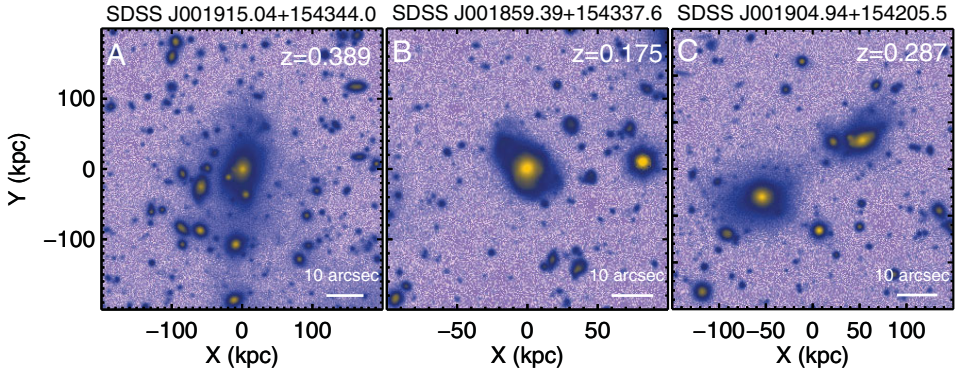

Figure 3. Zoom-in to some objects located around UGC 00180. Panel A shows a clusters of galaxies at z=0.389. Panel B and C illustrate the merging activity in a galaxy located at z=0.175 and a galaxy pair at z=0.287. Figure taken from Trujillo & Fliri (2016), reproduced by permission of the AAS.

of UGC 00180, this aperture is appropriate to probe features of 7.3×7.3 kpc. Values like that are typical of the FWHM of streams of nearby galaxies (e.g. Martínez-Delgado *et al.* 2008). Using square boxes of 10 arcsec×10 arcsec we obtain a surface brightness limit of 31.5 mag/arcsec^2 (3σ; r-band).

To construct the field of scattered light around UGC 00180 produced by the bright stars we need to accurately characterize the PSF of the image over an extension as large as possible. We conducted a campaign for observing with GTC (using the same rotation and dithering pattern than for the main object) the star γ Dra (V=2.36 mag). Such a

https://doi.org/10.1017/S1743921316009194 Published online by Cambridge University Press

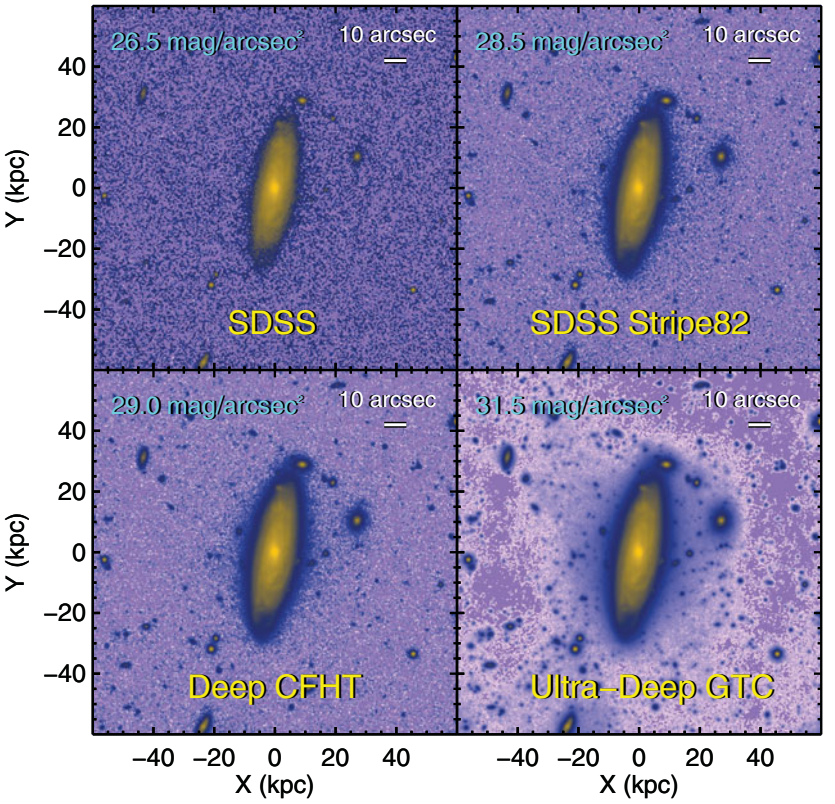

Figure 4. UGC 00180 as it would be observed by different surveys: SDSS, SDSS Stripe82, Deep data with CFHT and the present work. Figure taken from Trujillo & Fliri (2016), reproduced by permission of the AAS.

bright star allow us to explore the PSF of the GTC telescope down to a radial distance of ∼5 arcmin. With the PSF extremely well characterized down to large radial distances (error less than 0.28% at 5 arcmin) we construct the field of scattered light produced by the brightest (R<17 mag) stars of the image. UGC 00180 is placed in a region of the image where the contribution of the scattered light of the nearby brightest sources is rather homogeneous and around 29.2 mag/arcsec^2. After subtracting the scattered light distribution there is not any effect on the structure of the stellar halo around UGC 00180.

2.3. *The effect of the PSF on the surface brightness profile*

We simulate the effect of the PSF on the surface brightness distribution of our galaxy using the IMFIT code Erwin (2015). We select the following functions to fit the light distribution of our galaxy: a Sérsic (1968) bulge, a broken disk exponential (Erwin *et al.* 2008) and an exponential stellar halo. We convolve these functions with the PSF of the image and fit the galaxy light distribution. The convolved model is later on subtracted from the image to get the residuals of the fit. After that, we sum the residuals to the deconvolved IMFIT model to create an image of the galaxy with the effect of the PSF removed (Fig. 5).

The effect of the PSF on the galaxy light distribution is particularly relevant beyond 25 mag/arcsec^2 (r-band). The filamentary structure of the extra light surrounding UGC 00180 is also more evident once its light distribution is corrected by the effect of the PSF. The effect of the PSF on the surface brightness profile of the galaxy

https://doi.org/10.1017/S1743921316009194 Published online by Cambridge University Press

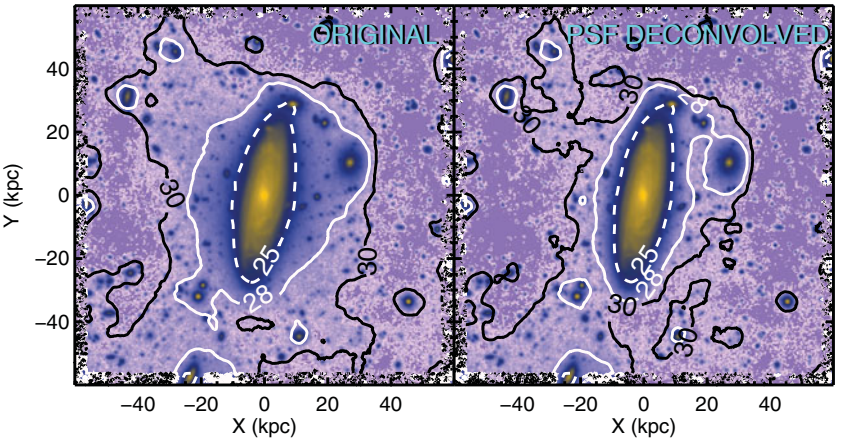

Figure 5. The figure shows the dramatic effect of the PSF on the surface brightness distribution of the galaxy. We indicate the position of the 25, 28 and 30 mag/arcsec^2 isophotes. Figure taken from Trujillo & Fliri (2016), reproduced by permission of the AAS.

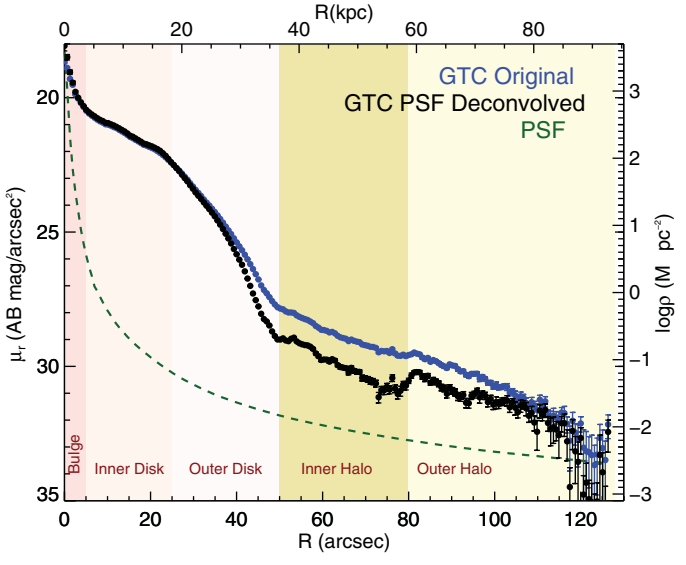

Figure 6. The effect of the PSF on the surface brightness profile of UGC 00180. The original profile is shown using blue points whereas the profile obtained after accounting by the effect of the PSF is plotted using dark points. The green dashed line shows the surface brightness profile of the GTC PSF. Figure taken from Trujillo & Fliri (2016), reproduced by permission of the AAS.

is illustrated on Fig. 6. The PSF affects both the central part, decreasing the central surface brightness of the bulge by ∼1 mag/arcsec^2 as well as the very outer region of the galaxy where the effect is the opposite. Beyond 25 mag/arcsec^2 the deconvolved profile starts to deviate from the original profile. At radial distances further than 50 arcsec, the difference between the original and the PSF corrected profile is around 1 mag/arcsec^2. This has important consequences on the analysis of the galaxy: the stellar halo region is much fainter (a factor of ∼2.5) than what it could be initially guessed using the original image of the galaxy.

https://doi.org/10.1017/S1743921316009194 Published online by Cambridge University Press

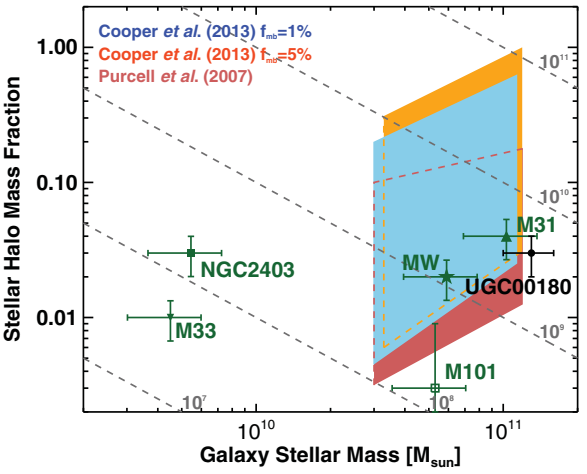

Figure 7. Stellar halo mass fraction versus total galaxy stellar mass. The figure shows the location of the stellar halos of galaxies compiled from the literature (green points) as well as the stellar halo of UGC 00180 (black solid point). In addition, we have overplotted the model predictions from Purcell *et al.* (2007) (red area) and Cooper *et al.* (2013) (blue and orange) for galaxies inhabiting dark matter halos with $12< \log_{10} M_{200}/M_{\odot} <12.5$. The grey dashed lines correspond to the positions on this plane of stellar halos with fixed stellar mass (10^7, 10^8, 10^9, 10^{10} and 10^{11} $M_{\odot}$). Figure taken from Trujillo & Fliri (2016), reproduced by permission of the AAS.

3. The stellar halo of UGC 00180

Motivated by the shape of the light distribution in Fig. 6, we model the stellar halo light distribution assuming an exponential profile. To allow a comparison of the stellar halo of UGC 00180 with other stellar halos reported in the literature, we assume that the ratio of the light contained in the stellar halo in the r-band is similar to the ratio of stellar mass. Figure 7 shows the stellar halo of UGC 00180 in comparison with other stellar halos measured in the literature: MW (Carollo *et al.* 2010), M31 (Courteau *et al.* 2011), M33 (McConnnachie *et al.* 2010), NGC2403 (Barker *et al.* 2012) and M101 (van Dokkum *et al.* 2014). It is worth noting that this result is only achievable when the effect of the PSF is taking into account. The amount of stellar mass contained in the stellar halo of UGC 00180 is around 4×10^9 $M_{\odot}$.

4. Summary

In this contribution we have shown that is feasible to reach 31.5 mag/arcsec^2 (3σ; 10×10 arcsec boxes in the r-band) with current largest optical telescopes using a reasonable amount of time: ∼8 hours on source. This is a surface brightness limit around 1.5-2 mag deeper than most current surveys dedicated to explore the faintest astronomical extended structures using integrated photometry. This limit is very close to what is currently achieved using the star count technique in nearby galaxies. The limiting surface brightness reached here shows that is possible to explore the stellar halos of distant galaxies and consequently test in-depth the predictions about the properties of the stellar halos provided by the ΛCDM galaxy formation scenario.

References

Abraham, R. G. & van Dokkum, P. G. 2014, *PASP*, 126, 55

https://doi.org/10.1017/S1743921316009194 Published online by Cambridge University Press

Barker, M. K., Ferguson, A. M. N., Irwin, M. J., Arimoto, N., & Jablonka, P. 2012, *MNRAS*, 419, 1489
Carollo, D., Beers, T. C., Chiba, M., *et al.* 2010, *ApJ*, 712, 692
Cooper, A. P., Cole, S., Frenk, C. S., *et al.* 2010, *MNRAS*, 406, 744
Cooper, A. P., D'Souza, R., Kauffmann, G., *et al.* 2013, *MNRAS*, 434, 3348
Courteau, S., Widrow, L. M., McDonald, M., *et al.* 2011, *ApJ*, 739, 20
Duc, P.-A., Cuillandre, J.-C., Karabal, E., *et al.* 2015, *MNRAS*, 446, 120
Erwin, P., Pohlen, M., & Beckman, J. E. 2008, *AJ*, 135, 20
Erwin, P. 2015, *ApJ*, 799, 226
Ferrarese L., *et al.* 2012, *ApJS*, 200, 4
Fliri, J. & Trujillo, I. 2016, *MNRAS*, 456, 1359
Ibata, R., Mouhcine, M., & Rejkuba, M. 2009, *MNRAS*, 395, 126
Jablonka, P., Tafelmeyer, M., Courbin, F., & Ferguson, A. M. N. 2010, *A&A*, 513, AA78
McConnachie, A. W., Irwin, M. J., Ibata, R. A., *et al.* 2009, *Nature*, 461, 66
Martínez-Delgado D., Peñarrubia J., Gabany R. J., Trujillo I., Majewski S. R., Pohlen M. 2008, *ApJ*, 689, 184
Martínez-Delgado D., *et al.* 2010, *AJ*, 140, 962
McConnachie, A. W., Ferguson, A. M. N., Irwin, M. J., *et al.* 2010, *ApJ*, 723, 1038
Mihos, J. C., Harding, P., Feldmeier, J., & Morrison, H. 2005, *ApJ*, 631, L41
Planck Collaboration, Ade, P. A. R., Aghanim, N., *et al.* 2014, *A&A*, 571, A1
Purcell, C. W., Bullock, J. S., & Zentner, A. R. 2007, *ApJ*, 666, 20
Sersic, J. L. 1968, Cordoba, Argentina: Observatorio Astronomico, 1968
Slater, C. T., Harding, P., & Mihos, J. C. 2009, *PASP*, 121, 1267
Trujillo, I. & Fliri, J. 2016, *ApJ*, 823, 123
van Dokkum, P. G., Abraham, R., & Merritt, A. 2014, *ApJ*, 782, L24
Zackrisson, E., de Jong, R. S., & Micheva, G. 2012, *MNRAS*, 421, 190

https://doi.org/10.1017/S1743921316009194 Published online by Cambridge University Press